Cellular Physiology and Biochemistry

Cell Physiol Biochem 2018;47:1565-1577
DOI: 10.1159/000490875
Published online: June 25, 2018
Accepted: May 14, 2018

Original Paper

Identification of Carbonic Anhydrase IX as a Novel Target for Endoscopic Molecular Imaging of Human Bladder Cancer

Jiaqi Wang[a] Ruizhe Fang[a] Lu Wang[a] Guang Chen[a] Hongzhi Wang[a] Zhichao Wang[a] Danfeng Zhao[a] Valentin N. Pavlov[b] Ildar Kabirov[b] Ziqi Wang[a] Pengyu Guo[a] Li Peng[a] Wanhai Xu[a]

[a]Department of Urology, the Fourth Hospital of Harbin Medical University, Harbin Medical University, Harbin, China, [b]Department of Urology, Clinic of Bashkir State Medical University, Ufa, Russia

Key Words
Endoscopic molecular imaging • Carbonic anhydrase IX • Bladder cancer • Blue-light cystoscopy • Fluorescent molecular

Abstract
Background/Aims: Emerging novel optical imaging techniques with cancer-specific molecular imaging agents offer a powerful and promising platform for cancer detection and resection. White-light cystoscopy and random bladder biopsies remain the most appropriate but nonetheless suboptimal diagnostic technique for bladder cancer, which is associated with high morbidity and recurrence. However, white-light cystoscopy has intrinsic shortcomings. Although current optical imaging technologies hold great potential for improved diagnostic accuracy, there are few imaging agents for specific molecular targeting. Carbonic anhydrase IX (CAIX) plays a pivotal role in tumorigenesis and tumor progression with potential value as an imaging target. Here, we investigated the feasibility of CAIX as a target and validated the diagnostic performance and significance of CAIX as an imaging agent. ***Methods:*** We first analyzed the data from The Cancer Genome Atlas (TCGA). Pairs of samples comprising bladder cancer and adjacent normal tissue were collected. All tissue samples were used for real-time PCR and immunohistochemistry to compare CAIX expression in normal and cancer tissue. Using blue-light cystoscopy, we observed the optical distribution of fluorescently labeled CAIX antibody in freshly excised human bladders and obtained random bladder biopsies to assess sensitivity and specificity. ***Results:*** The TCGA data revealed that CAIX expression was significantly higher in bladder cancer specimens than in normal tissue. The outcome was similar in quantitative real-time PCR analysis. In immunohistochemical analysis, bladder cancer specimens classified in four pathological subtypes presented a variety of positive staining intensities, whereas no benign specimens showed CAIX staining. Using blue-light cystoscopy, we distinguished bladder cancers that were mainly papillary, some variants of

J. Wang, R. Fang and L. Wang contributed equally to this work.

Wanhai Xu, MD, PhD
Department of Urology, The Fourth Hospital of Harbin Medical University
Yiyuan Street NO.37, Harbin, 150001 (China)
Tel. +86-045185939377, E-Mail xuwanhai@hrbmu.edu.cn

urothelial carcinoma, and less carcinoma in situ, from benign tissue, despite the presence of suspicious-appearing mucosa. The sensitivity and specificity for CAIX-targeted imaging were 88.00% and 93.75%, respectively. ***Conclusions:*** CAIX-targeted molecular imaging could be a feasible and adaptive alternative approach for the accurate diagnosis and complete resection of bladder cancer.

Introduction

Optical imaging techniques used for interventional guidance have evolved rapidly in recent years. Likewise, more and more cancer-specific targets have been identified as promising molecular imaging agents. The combination of the advances in both of these areas has permitted powerful and useful alternatives or adjuncts to traditional means of endoscopic cancer detection and resection [1, 2]. White-light endoscopy is the technique primarily used to optically inspect cancers of the gastrointestinal and urinary tracts for subsequent biopsy or resection [3]. However, although it is the gold standard for the diagnosis of some solid tumors, the complete extent of the tumor burden of a local organ can be difficult to confirm on white-light endoscopy alone, particularly for small "satellite" tumors or areas of early lesions that appear flat with unclear boundaries. Inadequate visualization of microtumors on white-light endoscopy could account for cancer recurrence and progression. However, fluorescent endoscopy with fluorescently labeled molecular probes offers enhanced differentiation between tumors and adjacent normal or benign tissues. Therefore, exploration of molecular imaging agents that can specifically target cancer is of considerable interest.

In 2017, there were an estimated 80, 000 cases of bladder cancer (BC) in the United States, making BC the second most common malignancy of the urinary system [4]. This cancer has high recurrence, up to 50–70% at 5 years for non-muscle-invasive BC (NMIBC) [5]. Because the recurrence rate requires intensive endoscopic surveillance strategies or additional operations, BC management is the most expensive of all solid tumors [6]. White-light cystoscopy and random bladder biopsies for pathological diagnosis and local staging remain the most appropriate techniques for the diagnosis and follow-up of BC. Approximately 75% of urinary bladder tumors are superficial NMIBC. For these patients, endoscopic resection followed by intravesical Bacillus Calmette–Guérin (BCG) vaccine or chemotherapy is recommended for definitive treatment, whereas multiple treatments involving radical cystectomy with neoadjuvant chemotherapy is the standard treatment strategy for patients who present or recur with muscle-invasive cancer (stage ≥ T2) [7, 8]. However, white-light cystoscopy has some well-known deficiencies, including inadequate tumor delineation to enable complete resection (especially for carcinoma in situ [CIS]) and difficult differentiation between inflammation and malignancy [9].

In recent years, novel molecular imaging technologies used to identify suspicious lesions have sprung up rapidly, such as fluorescence cystoscopy/photodynamic diagnosis, narrow band imaging, and confocal laser endomicroscopy, which aim to address the limitations of white-light cystoscopy and have *in vivo* feasibility [10]. Blue-light cystoscopy with various photosensitizers, such as hexaminolevulinate hydrochloride (HAL), as a promising adjunct to white-light cystoscopy for enhanced identification and guidance of endoscopic resection takes advantage of the preferential uptake and accumulation of protoporphyrins in neoplastic tissue, which emit a red fluorescence when excited using blue light (360–450 nm wavelengths) [11]. However, there are still limitations to its clinical application. The operators require considerable experience to distinguish false-positive fluorescence from unspecific uptake of protoporphyrins by inflammatory lesions. Additionally, further work showed fewer benefits for tumor detection [10].

In this study, we aimed to use a cancer-specific imaging agent to develop a targeted molecular imaging strategy to overcome the defects of current visualizing imaging technologies. We considered carbonic anhydrase IX (CAIX) to be of interest after investigating published work [12-15] and analyzing the data of preliminary experiments. Functionally,

CAIX plays an important role in the acid-base homeostasis of tumors under hypoxic conditions due to the deleterious effects of a high rate of glycolytic metabolism in tumor sites. This can lead to more aggressive and treatment-resistant tumor phenotypes [12]. Therefore, the inhibition of CAIX with a relevant antibody could allow the use of an extensive therapeutic strategy to suppress tumor growth and reduce metastasis in cancer patients. Previous studies demonstrated that CAIX is an ideal biomarker for tracking the recurrence, progression, and overall survival of BC patients [13-15]. Not only is CAIX constitutively expressed in most BCs, but it is also expressed differentially in noninvasive versus invasive tumors, in low-grade versus high-grade BC, and in primary tumors versus metastases [13-15]. Considering the differential expression and function of CAIX, we developed and evaluated a fluorescently labeled antibody (anti-CAIX) as an intravesical imaging agent for optimizing the integration of novel imaging technologies into clinical practice.

Materials and Methods

Human tissue samples

Human BC tissues were provided by the Fourth Affiliated Hospital of Harbin Medical University after approval was obtained from the university's Ethics Committee on the Use of Human Samples. The tissues were obtained from 8 individuals undergoing radical cystectomy. The sampled tissues were immediately snap-frozen in liquid nitrogen and stored at –80°C.

Identification of differentially expressed genes associated with BC

Based on the edgeR algorithm, we identified differentially expressed genes (DEGs) with mRNA expression profiles. The Benjamini-Hochberg multiple testing method was used to adjust the p value (false discovery rate [FDR]). The thresholds were FDR < 0.01 and |log2FC| > 2 (FC, fold change). We considered the genes satisfying these criteria to be DEGs.

Real-time PCR

Total RNA was extracted from the human tissues and cell lines using Trizol (Invitrogen, Carlsbad, California, USA). The levels of CAIX mRNA were quantified using the mirVana quantitative real-time PCR (qRT-PCR) miRNA Detection Kit (Ambion, Carlsbad, California, USA) in conjunction with real-time PCR with SYBR Green I (Applied Biosystems, Carlsbad, California, USA) according to the manufacturer's instructions. The qRT-PCR was performed on an ABI Prism® 7500 fast thermocycler (Applied Biosystems) for 40 cycles. The following CAIX primers were used for PCR detection: 5'-GGGAGGTGGTCGCTGTAAAA-3' (forward), 5'-ACCAGCACTGTAGCACACTC-3' (reverse). The relative expression levels of CAIX were calculated through normalization to their internal control (glyceraldehyde 3-phosphate dehydrogenase [GAPDH]). The relative expression intensity values were calculated as $2^{-\Delta\Delta Ct}$.

Immunohistochemical staining

Tissue samples were fixed in 4% formaldehyde and embedded in paraffin. For the immunohistochemical study, the deparaffinized tissue sections were incubated with affinity-purified antibodies against CAIX (1:200) as the primary antibody. Immunoperoxidase staining was applied to the specimens using the streptavidin-biotin-peroxidase complex. The samples were classified as CAIX-negative or CAIX-positive according to whether the percentage of CAIX-positive cells was <10% or >10%, respectively. And all the IHC slides were analyzed by Image Pro Plus 6.0 through calculating the integrated optical density (IOD) value of staining parts

CAIX fluorescent imaging by blue-light cystoscopy

Anti-CAIX antibody was labeled with Qdot625 (excitation, 405 nm; emission, 625 nm; Life Technologies) by amine-thiol cross-linking per the manufacturer's protocol. The labeled antibody (15 nM in 50 mL saline) was instilled into fresh intact bladders and incubated for 1 h. For imaging, all of the bladder specimens were treated with a clinical blue-light cystoscopy system (Karl Storz) that is able to shift between standard white light and blue light for fluorescence imaging (375 to 440 nm) and detection of red light above 610 nm [11].

A tangential angle of incidence of blue light to bladder mucosa may demonstrate false-positive findings. Positive anti-CAIX-Qdot625 fluorescence was defined as a discrete area with sustaining pink fluorescence independent of distance and angle of observation. True positive was defined as a histologically confirmed BC that showed pink fluorescence under blue light. True negative was defined as histologically confirmed benign mucosa (e.g., normal, inflammation) with background blue fluorescence. And the fluorescent intensity was quantified by mean densities (IOD/Area) of sustaining pink parts.

Statistical analysis

All data are presented as the mean ± standard error of the mean. A t-test using Bonferroni correction or a Dunnett's test was used to evaluate the significance of the differences between the individual means. Otherwise, the data were compared by a Student's t-test. A two-tailed difference with $p < 0.05$ was considered statistically significant. For the diagnostic accuracy of CAIX-targeted blue light cystoscopy imaging, sensitivity was calculated as TP/(TP + FN), and specificity as TN/(TN + FP), (TP: true positive, FN: false negative, TN: true negative, and FP: false positive). 2-tailed Spearman's correlation coefficient method was used to assess correlation between two parameters. The data were analyzed using GraphPad Prism 7.0.

Results

CAIX expression

Some studies have reported that CAIX expression is markedly higher in urine samples from BC patients compared with controls [14, 15]. In this context, we hypothesized that CAIX expression would be significantly different between BC and normal tissue specimens. Therefore, we designed a scientific and systematic validation process to explore the differential expression of CAIX between BC tissue and normal bladder tissue. We first focused on the analysis of data from The Cancer Genome Atlas (TCGA) and performed a whole-genome expression analysis in 410 tumor tissues and 19 normal tissues from patients with BC using the R package edgeR. The Benjamini-Hochberg multiple testing method was used to correct the p values.

Using the criteria (|log2FC|>2, FDR<0.01), 1156 DEGs were assigned to the BC group. About two-fifths of the total DEGs were overexpressed in cancer tissue (446 genes, 39% [cancer] > [normal]), whereas the others exhibited reduced expression (710 genes, 61% [normal] > [cancer]) (Fig. 1A). We next analyzed the expression of CAIX in the same data set. CAIX expression was significantly higher in the BC specimens than in normal tissue (Fig. 1B).

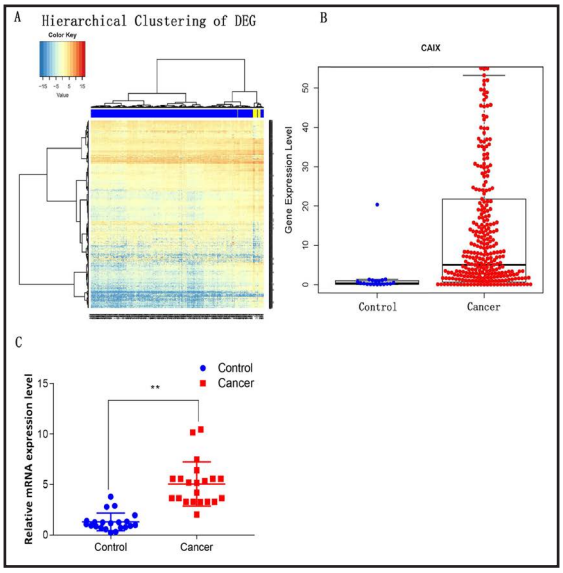

Fig. 1. Identification and analysis of differentially expressed genes (DEGs) and CAIX expression. (A) Hierarchical clustering of DEGs, with rows representing genes and columns representing samples. For a gene, red represents a higher expression level, blue represents a lower expression level, and white represents the median expression level for all samples. For a sample, yellow means tumor-adjacent tissues and blue means tumor tissues from patients with BC. (B) CAIX expression levels in the BC (n = 410) group and normal group (n = 19) (|log2FC|>2, FDR<0.01). (C) Relative CAIX mRNA expression was quantified by qRT-PCR in 21 matching samples of bladder cancer and adjacent normal tissue. GAPDH was used as a loading control. p<0.01, n = 21.

To further confirm the differential expression of CAIX, 21 matching samples of BC and adjacent normal tissue were obtained from patients who underwent cystectomy or transurethral resection of the bladder (TURB). All of the associated clinical and pathologic information were also prospectively collected from the BC patients (Table 1). Total RNA was isolated from all of the selected fresh snap-frozen specimens. The expression of CAIX was analyzed by qRT-PCR after reverse transcription. A 3.9-fold increase in CAIX mRNA expression was detected in the BC tissue compared with the control ($p < 0.01$) (Fig. 1B).

To assess the expression of CAIX, 18 paraffin-embedded BC specimens covering five pathological subtypes (noninvasive papillary urothelial carcinoma, urothelial carcinoma, papillary urothelial carcinoma with squamous differentiation, CIS, and adenocarcinoma) were subjected to an immunohistochemical assay with affinity-purified antibodies against CAIX. In addition, 9 specimens of benign bladder tissue including normal mucosa, squamous metaplasia, and inflammation were also considered. BC specimens classified in four pathological subtypes presented a variety of positive staining intensities, whereas all the benign specimens showed negative (Fig. 2A–I). And it was demonstrated differential expression of CAIX between bladder cancer and benign bladder tissues ($p<0.01$, Fig 2J). Remarkably, even high grade papillary UCs that had the lowest level CAIX staining in all types of bladder cancer showed significant increase

Table 1. Patient and Tumor Characteristics

Variable	No. of patients (%)
Sex	
Men	13 (61.9)
Women	8 (38.1)
Median age [range], y	69 [53–81]
Operation type	
Cystectomy	2 (9.5)
TURB	19 (90.5)
Tumor stage	
pTa	1 (4.8)
pT1	13 (61.9)
pT2	4 (19.0)
pT3	2 (9.5)
pT4	1 (4.8)
Tumor grade	
G1	8 (38.1)
G2	11 (52.4)
G3	2 (9.5)
Metastasis at diagnosis	0 (0.0)
Non-metastasis at diagnosis	21 (100.0)
Dead	0 (0.0)

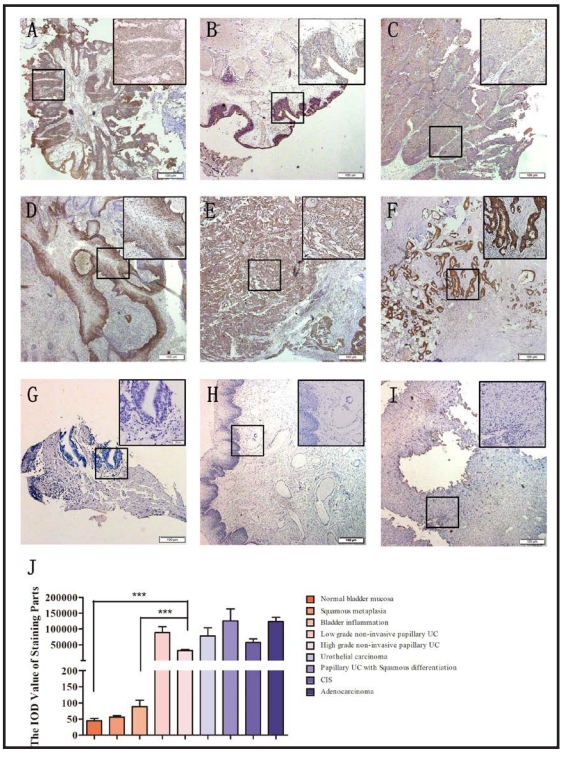

Fig. 2. Immunohistochemical staining patterns for different pathological subtypes of bladder cancer and benign bladder tissue. Mouse monoclonal affinity-purified anti-CAIX antibodies and anti-mouse IgG peroxidase conjugate were used to visualize CAIX-positive cells in paraffin sections. (A) Low-grade noninvasive papillary urothelial carcinoma, (B) high-grade noninvasive papillary urothelial carcinoma, (C) urothelial carcinoma, (D) papillary urothelial carcinoma with squamous differentiation, (E) CIS, (F) adenocarcinoma, (G) normal bladder mucosa, (H) squamous metaplasia, and (I) bladder inflammation. (J) the quantification of CAIX staining for different pathological subtypes of bladder cancer and benign bladder tissue. In order from the left to right: normal bladder mucosa, squamous metaplasia, bladder inflammation, low-grade noninvasive papillary urothelial carcinoma, high-grade noninvasive papillary urothelial carcinoma, urothelial carcinoma, papillary urothelial carcinoma with squamous differentiation, CIS, adenocarcinoma. (Low-grade noninvasive papillary UC vs normal bladder mucosa and bladder inflammation, $p<0.01$). Magnification: ×100. Scale bars, 100 μm.

in CAIX expression compared with the adjacent normal bladder tissues. Consistent with our findings, an article published in European Urology [14] has shed further light on the significant difference in CAIX expression between paired urine and tumor specimens. All of the data suggest the promising value of CAIX as a targeted molecular imaging agent for BC.

Table 2. Patient and Associated Clinicopathologic Characteristics

Variable	No. of patients (%)
Sex	
Men	5 (82.5)
Women	3 (37.5)
Median age [range], y	71 [69–81]
No. of tumors	
1	3 (37.5)
≥2	5 (62.5)
Tumor stage	
pT2	1 (12.5)
pT3	4 (50.0)
pT4	3 (37.5)
Tumor grade	
Low	0 (0.0)
High	8 (100.0)
Metastasis at diagnosis	1 (12.5)
Non-metastasis at diagnosis	7 (87.5)
Recurrence during FU	1 (12.5)
Progression during FU	0 (0.0)

Application of CAIX to in vivo endoscopy molecular imaging

Blue-light cystoscopy is characterized by the combination of white-light cystoscopy and a blue-light fluorescence-exciting system, which allow the operator to switch dynamically between them. To evaluate the value of anti-CAIX as a BC imaging agent *in vivo*, we developed an endoscopic molecular imaging protocol for the human bladder. Considering the possibility of latent toxicity and unexpected adverse events in associated with *in vivo* examination of the bladder, we obtained fresh, intact bladder from patients with high-stage muscle-invasive BC or multiple high-risk NMIBC who underwent radical cystectomy (n = 8). The clinicopathologic characteristics of the patients with BC are shown in Table 2. Next, we linked the monoclonal CAIX antibody with a fluorescent molecule (Qdot625) and intravesically instilled the labeled anti-CAIX via a catheter. After antibody binding for one hour, the excess antibody was removed by irrigation of the bladder with normal saline. The bladders coated with fluorescent-labeled antibody were imaged with blue-light cystoscopy.

BC specificity by targeting CAIX

To clarify whether the pink fluorescence emitted by cancer lesions is attributable to the cancer-specific binding of anti-CAIX-Qdot625, we first incubated a single bladder with Qdot625-labeled isotype control (IgG-Qdot625). After one hour for binding the bladder was voided and washed. We expected that there would be no pink fluorescence on the whole bladder mucosa regardless of the presence of cancerous or normal tissue under blue-light cystoscopy. Then, we reincubated the bladder with Qdot625-labeled anti-CAIX for one hour and obtained intravesical images of the bladder using cystoscopy. Observation under blue-light cystoscopy revealed that there was pink fluorescence on the mucosae with malignant features, but not on normal mucosae, indicating CAIX specificity. Subsequent histopathology of biopsy tissue showed that the lesion binding the anti-CAIX-Qdot625 contained papillary urothelial carcinoma, whereas the region without anti-CAIX-Qdot625 binding contained normal urothelium (Fig. 3A).

Diagnostic accuracy of CAIX-targeted imaging

To assess the diagnostic value of the novel fluorescent-labeled agent, we performed cystoscopy in all of the excised bladders (n = 8). White- and blue-light images were obtained of benign and cancerous regions after incubation with anti-CAIX-Qdot625 (Fig. 3B&C). In total, 57 biopsies, including bladder tumor-appearing areas, flat suspicious lesions, and normal bladder mucosa, were examined under white-light cystoscopy, and all fluorescent sites were viewed under blue-light cystoscopy (Table 3&4). Furthermore, all biopsies were verified by histopathological diagnosis. The malignant pathological outcomes included noninvasive papillary urothelial carcinoma (low grade and high grade), CIS, and infiltrating urothelial carcinoma, whereas the benign outcomes were inflammatory tissue and normal urothelium.

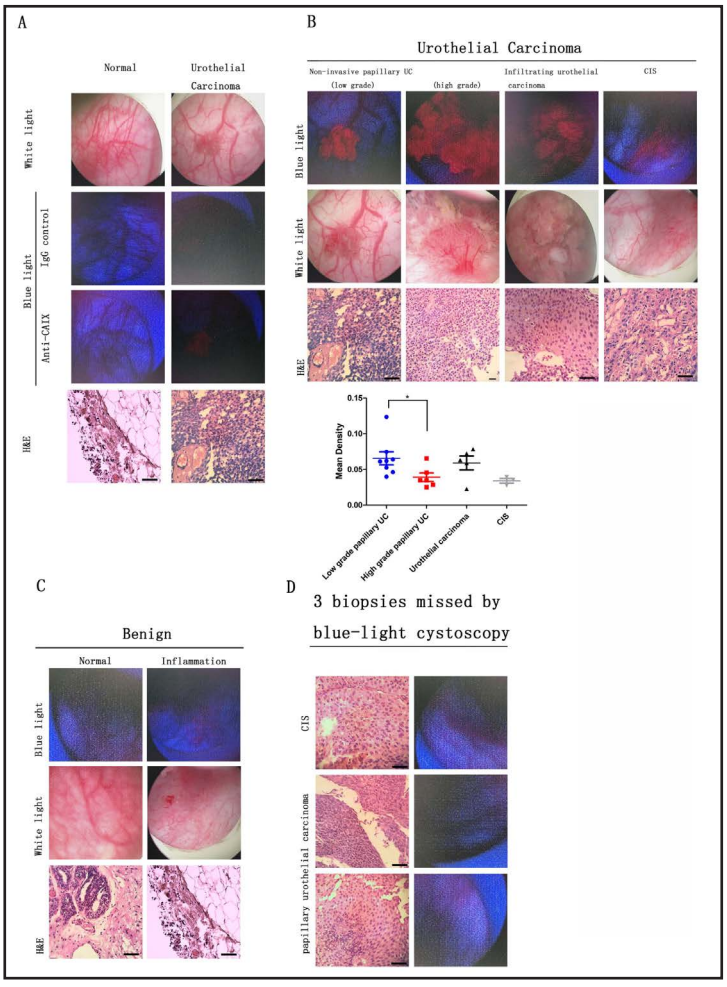

Fig. 3. Blue cystoscopic molecular imaging of human bladder cancer using Qdot625-labeled CAIX antibody. Representative white and blue-light images with the relevant hematoxylin and eosin-stained photomicrographs for co-localization of anti-CAIX-Qdot62 binding and histopathology. (A) To verify cancer-specific binding of fluorescent antibody, intravesical instillation of a single bladder was first performed with IgG control-Qdot625 and imaged under white and blue light and then re-incubated with anti-CAIX-Qdot62 and imaged. White- and blue-light images of normal mucosa and a noninvasive papillary urothelial carcinoma after incubation with the two antibodies are shown. (B and C) Representative white- and blue-light images of benign and cancerous regions after incubation with anti-CAIX-Qdot625. (B) Visual fluorescence was detected under blue light (upper panel), including low-grade noninvasive papillary urothelial carcinoma, high-grade noninvasive papillary urothelial carcinoma, urothelial epithelial carcinoma, and CIS. The fluorescent graphs were quantified by mean densities (IOD/Area) of red part of each one shown in statistical graph (lower panel). (C) Benign regions of normal urothelium and inflammation show no detectable fluorescent signal. (D) The blue-light and HE picture of 3 biopsies of tumors that were not identified by blue-light cystoscopy. Scale bars, 50 μm.

In total, 22 of 25 biopsies pathologically confirmed as cancer were true positive in terms of fluorescence, indicating a sensitivity of 88.00%, whereas the remaining 3 biopsies had no evidence of anti-CAIX binding, suggesting a 12.00% missed diagnosis rate. The 3 biopsies that were not identified by blue-light cystoscopy were respectively diagnosed by pathology as papillary urothelial carcinoma (2

Table 3. Comparison of CAIX-targeted imaging analysis using blue-light cystoscopy with histopathological diagnosis. Tumor-appearing, suspicious flat lesion, and normal bladder mucosa were biopsied for histopathological diagnosis. The overall sensitivity was 88.0% and the specificity was 93.75% for CAIX-targeted imaging of bladder cancer

Histpathological Diagnosis	No.of biopsies	Median Age	CAIX-Targeted Imaging			
			True Positive	False Positive	Ture Negative	False Negative
Cancer						
Cancer Total	25	71	22			3
• Non-invasive papillary UC	16	75	14			2
• Infiltrating UC	5	69	5			0
• CIS	4	72	3			1
Benign						
Benign Total	32	71		2	30	
• Normal Urothelium	26	71		1	25	
• Inflammation	6	73		1	5	

biopsies) and carcinoma in situ (1 biopsy) (3D). The fluorescent graphs were quantified by mean densities (IOD/Area) of sustaining pink parts shown in Fig. 3C.

From the 32 benign tissues validated by pathology, 30 biopsies were true negative without detectable anti-CAIX binding, giving a specificity of 93.75%. However, the 2 misdiagnosed biopsy that appeared to be benign under blue-light cystoscopy were pathologically confirmed as normal urothelium and inflammatory lesion (1 each).

It is easy to differentiate papillary urothelial carcinoma from normal urothelium by conventional white-light cystoscopy. Noninvasive papillary urothelial carcinoma is the most common type of BC, accounting for 75% of BCs. Notably, 12 of the 14 biopsies pathologically diagnosed with this condition showed the pink fluorescence of anti-CAIX-Qdot625. Similarly, 5 of the 5 biopsies with pathologically confirmed infiltrating urothelial carcinoma also presented positive anti-CAIX-Qdot625 signal.

Table 4. Comparison of imaging analysis using white cystoscopy with histopathological diagnosis. The overall sensitivity is 76.0% and a specificity is 96 .75% for white-light cystoscopy imaging of bladder cancer

Histpathological Diagnosis	No.of biopsies	Median Age	CAIX-Targeted Imaging			
			True Positive	False Positive	Ture Negative	False Negative
Cancer						
Cancer Total	25	71	19			6
● Non-invasive papillary UC	16	75	14			2
● Infiltrating UC	5	69	5			0
● CIS	4	72	0			4
Benign						
Benign Total	32	71		1	31	
● Normal Urothelium	26	71		0	26	
● Inflammation	6	73		1	5	

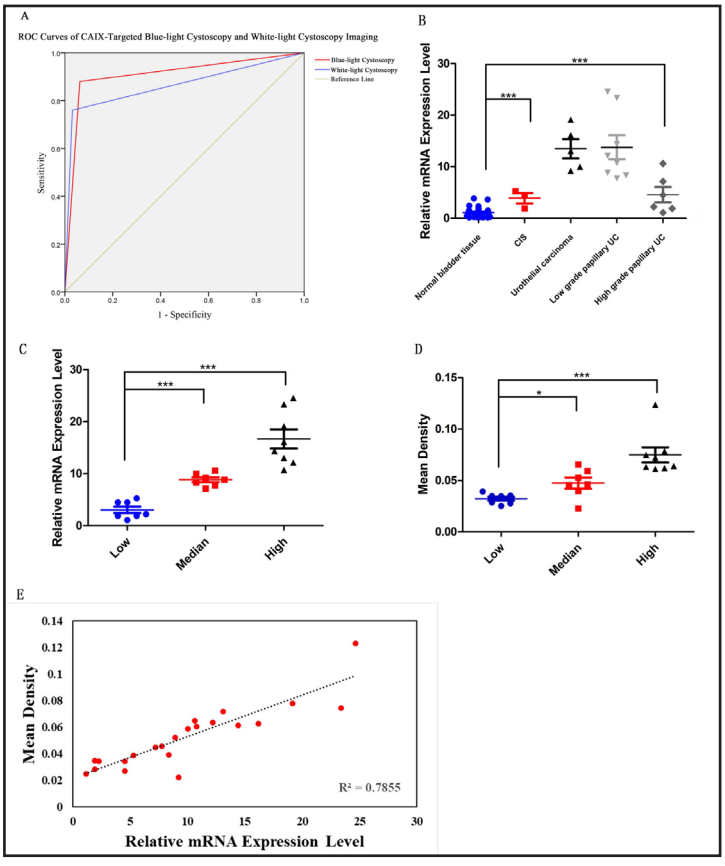

Fig. 4. The diagnostic accuracy of CAIX-targeted blue-light cystoscopy. (A) ROC curve illustrating the diagnostic accuracy of the two imaging methods for identifying bladder cancer. Curves are presented for CAIX-targeted blue-light cystoscopy (red line) and white-light cystoscopy imaging (blue line). (B) the relative CAIX expression level of 22 tumor biopsies which were detected by blue-light cystoscopy. Extra 26 samples of normal bladder were control group (all groups vs control, $p<0.01$). (C) the relative CAIX expression level of three group (low expression, median expression, high expression, median group vs high group, $p<0.01$). (D) the mean density conforming to above grouping. (median group vs high group, $p<0.05$) (E) Showing positive correlation between CAIX expression and fluorescent intensity under blue-light cystoscopy in 22 bladder cancer tissues (2-tailed Spearman's correlation, r=0.886, p<0.01).

CIS generally appears as flat lesions that are hardly visible on ultrasound, computed tomography, or magnetic resonance imaging. These lesions have high risk of progression to muscle-invasive cancer and recurrence. Even when comprehensively examined by white-light cystoscopy, some CISs still cannot be distinguished from the normal urothelium due to its high resemblance to normal mucosa and its indistinct margins. For the group of CISs, 3 of the 4 were detected by blue-light cystoscopy through anti-CAIX-Qdot625 imaging. Notably, all CIS biopsies showed normal appearance under white-light cystoscopy and were overlooked but could be seen when imaged under blue light.

For suspicious benign lesions and normal urothelium under white light, 5 of the 6 inflammatory lesions without anti-CAIX-Qdot625 binding were classified in the true negative group. Except for one site of the normal bladder mucosa that showed a slight fluorescent signal, the remaining 25 sites displayed only blue background and vascular venation. Although inflammation is likely to bind anti-CAIX-Qdot625 due to denudation of the urothelium or lymphocyte infiltration, 96.15% of these benign biopsies were true negative for anti-CAIX-Qdot625 binding (Table 3). And ROC curve was plotted to illustrate the diagnostic accuracy of the two imaging methods for identifying bladder cancer (Fig 4A). We further detected CAIX expression of 22 tumor biopsies which were found by blue-light cystoscopy (Fig 4B) and divided them with three groups according to expression level (low, median, and high expression, 33% and 66% as cutoff point of the expression data in ascending order) (Fig 4C). And after analyzing the mean density of each corresponding graph we found the differences of mean density between three groups also were statistically significant (low vs median, $p < 0.05$, low vs high, $p < 0.01$) (Fig 4D). By using Spearman's correlation coefficient method, we got positive correlation between CAIX expression and fluorescent intensity under blue-light cystoscopy ($r=0.886$, $p < 0.01$) (Fig 4E). In summary, the anti-CAIX-Qdot625 guided blue-light cystoscopy showed the higher sensitivity compared with white-light cystoscopy imaging conferred more precise detection of small lesions.

Discussion

Significant attention has been paid to fluorescence guidance of the diagnosis and surgical resection of BC due to potential improvements in sensitivity and specificity and the long-term benefits for recurrence and progression after resection. In this study, we endeavored to develop a novel endoscopic imaging system involving blue-light cystoscopy by combining a fluorescent imaging agent that targeted CAIX, a surface protein with differential expression between cancer cells and normal urothelium. Our work demonstrated that the high expression of CAIX in BC makes it a viable imaging target. We successfully developed a CAIX antibody labeled with a fluorescent tag, anti-CAIX-Qdot625, for intravesical administration. Detection of anti-CAIX bound to the luminal surface of biopsy tissue from tumors but not normal tissue supports the specific targeting of CAIX via intravesical administration of the antibody. In addition, we used a whole-bladder imaging strategy to simulate a future *in vivo* endoscopic application and facilitate clinical translation of the anti-CAIX molecular imaging in order to improve BC detection and transurethral resection quality.

Cancer cells tend to grow under hypoxic conditions and shift their metabolism from a high level of glycolysis to lactic acid fermentation in the cytoplasm [16]. CAIX, as a transporter of CO_2 and hydrogen carbonate, is believed to export and extrude H^+ out of the cytosol to maintain the intracellular physiological pH homeostasis. In addition, the expression level of CAIX is significantly related to the hypoxic status [17]. Extensive research has shown that an elevated expression of CAIX is often related to poor prognosis in many malignancies, including renal cell carcinoma, breast, cervical, and non-small cell lung cancer, as well as BC [18-21]. In renal cell carcinoma, expression of CAIX is controlled by the lack of or an aberration in von Hippel-Lindau (VHL), a tumor-suppressing gene, and nearly all forms of clear cell renal cell carcinoma express high levels of CAIX, which is downregulated in normal kidney tissue [22]. Thus, CAIX is a tumor-associated antigen cancer with diagnostic utility

in identifying carcinoma and benign tissue. In this context, we successfully validated the discrepancy at both the mRNA and protein level, offering evidence on the feasibility of this cancer-specific fluorescent imaging agent.

Blue-light cystoscopy, also called fluorescence cystoscopy or photodynamic diagnosis, is a technique based on white-light cystoscopy that provides clearer imaging of BC. A meta-analysis including 1345 patients found that blue-light cystoscopy identified significantly more Ta-T1 tumors (14.7%; $p < 0.001$; odds ratio, 4.90; 95% confidence interval, 1.94–12.39) and CIS lesions (40.8%; $p < 0.001$; odds ratio, 12.372; 95% confidence interval, 6.34–24.13) than white-light cystoscopy and contributed to lower 12-month recurrence rates in patients with T1 cancer or CIS [23]. Previously, the advent of new photosensitizers led to considerable attention to blue-light cystoscopy amid the possibility of numerous applications. In addition, endoscopic molecular imaging with photosensitive protoporphyrin analogues takes advantage of the selective accumulation abilities of rapidly proliferating cells. Most clinical studies of photosensitive protoporphyrin analogues are based on 5-ALA [24], although another analogue, HAL, is more promising, given that it has been approved for clinical use in both Europe and the United States [11]. Although the approved photodynamic diagnosis based on protoporphyrins such as hexaminolevulinate shares the advantages of an improved detection of NMIBC beyond that achieved with white-light cystoscopy, there are several inherent and technical deficiencies that restrict the extensive clinical application of photodynamic diagnosis with protoporphyrin. Up to a 30% false-positive rate has been reported, particularly with prior BCG treatment or chemotherapy that lead to overuse of bladder biopsies due to low surgeon experience in the learning period [25]. Other possible reasons for false-positive findings include autofluorescence, which is caused by activation of the endogenous fluorescence in response to the blue light and tangential imaging [9, 26]. Hexaminolevulinate is approved for single administration on account of potential drug hypersensitivity with repeat exposure. Other technical limitations include a decreased optical management with incomplete hemostasis and a photobleaching effect causing loss of fluorescence [27]. Undeniably, wide-field fluorescence imaging of CAIX offers potential advantages over the currently approved blue-light cystoscopy with protoporphyrin.

Our results showed that anti-CAIX-Qdot625 binds to papillary urothelial carcinoma regardless of grade and the presence of infiltrating urothelial carcinoma. Anti-CAIX fluorescent imaging also overcame the diagnostic limitation of white-light cystoscopy, competently identifying CIS, which is missed by white-light cystoscopy. BCG is still the most effective intravesical treatment to decrease both the progression and recurrence of high-risk nonmuscle-invasive bladder cancers, including CIS [28, 29]. In addition to BCG, a growing number of studies have investigated alternative intravesical agents with equivalent efficacy to BCG [30]. We believe that CAIX imaging may improve CIS identification and better stratify patients who would benefit most from BCG treatment while evaluating the treatment response to BCG. In further study, more pathological types of BC should be included, such as papillary urothelial carcinoma with squamous differentiation, micropapillary carcinoma, and adenocarcinoma. All of these pathological types present infrequently in patients with BC and thus require long-time specimen collection periods.

The bladder is a hollow organ with an established intravesical route to receive and reserve pharmacological agents including live attenuated vaccines (e.g., BCG) and high-dose chemotherapy (e.g., gemcitabine) without significant systemic absorption. Its unique physiological and anatomic properties allow intravesical administration, which minimizes potential systemic toxicity from the imaging agent, making the bladder an attractive target organ for endoscopic molecular imaging and image-guided surgery. The CAIX antibody used in our study is a mouse monoclonal antibody and unlikely to be suitable for application to humans due to the risk of an allergic response caused by heterogeneous serum. However, a humanized, compatible manufacturing practice-grade monoclonal CAIX antibody is currently being studied for therapeutic use. A novel human anti-CAIX monoclonal antibody has therapeutic potential in the unmet medical need of the specific elimination of highly-expressed CAIX renal carcinoma cells [31]. In addition, the chimeric antibody girentuximab

has been widely tested in clinical trials for administration both alone and in combination with multiple drugs, including radioisotopes, cytokines, and chimeric antigen receptor (CAR) T cell therapy [32, 33]. If the CAIX antibody is found to be safe without toxic side-effects *in vivo*, it could be labeled with a fluorescent molecule for optical molecular imaging. Even if this CAIX antibody is not suitable for systemic administration, the intravesical mode allows a safe alternative for diagnosis and treatment.

For the clinical translation of a Qdot625-labeled CAIX antibody, additional work is required to determine the stability and safety profile of intravesical anti-CAIX before human trials. Quantum dots (Qdots), which are semiconductor nanocrystals ranging from 2 to 10 nm in diameter, are promising alternatives to organic dyes, which emit fluorescence depending on their particle size [34]. Despite the latent toxicity of the heavy metal core in Qdots, considerable effort is being expended to improve their biocompatibility and stability, given the advantages of Qdots, including stronger fluorescence intensity and resistance to photobleaching upon excitation.

Although our study indicated that CAIX as an imaging target is an important predictor of overall survival and that CAIX-targeted imaging allows detection of a wide variety of BC types, there are other putative intrinsic markers of hypoxia under regulation by hypoxia-inducible factor-1 (HIF-1). Studies have indicated that HIF-1α fused to firefly luciferase can be used to dynamically monitor cardiomyocyte oxygenation in living heart muscle samples [35]. In addition to HIF-1α, studies have shown that GLUT1 expression is absent from normal bladder mucosa but is present in malignant bladder mucosa, with greater expression in muscle-invasive tumors compared with superficial BC [36]. Li et al. [37] reported that miR-218 increases the sensitivity of BC to cisplatin, an effect that can be ameliorated by targeting GLUT1, indicating its potential therapeutic value. CD44, a member of the cell surface glycoprotein family, functions in cell-cell and cell-matrix interactions, chiefly in epithelial cells [38]. CD44 and its variants are closely related to aggressive progression and poor patient prognosis in many types of cancer [39, 40]. BCs progressively lose CD44 proteins as they penetrate deeper and become less differentiated. In patients lacking CD44v6 in BC tissue, there is a 2.3-fold increased risk of recurrence (95% confidence interval, 1.28–4.08) [41]. Pan et al. [42] reported CD47 as a target for blue-light cystoscopy imaging of BC. The study found a sensitivity of 82.9% and a specificity of 90.5% for CD47-targeted imaging of BC. Although several promising candidate markers such as CAIX have been identified, there are few potent molecular biomarkers with widely proven utility for endoscopic molecular imaging in general and for improving clinical outcomes. Identification of molecular markers that better classify tumors with multiple tumor characteristics such as the pathological stage or response to specific treatment may help in the development of more refined imaging detection tools for the selection of precise and individualized BC therapies.

Our research sheds new light on the identification and validation of molecular imaging targets, with CAIX serving as a cancer-specific imaging agent for BC and likely for other epithelial cancers. Our intact-organ imaging approach takes advantage of the ease of accessing the well-established intravesical route of the bladder for drug administration. This imaging system represents a potentially powerful way to facilitate the endoscopic detection of cancer and its resection in the urinary bladder or other hollow viscera, contributing to better overall survival due to less recurrence. Together, our study offers sufficient evidence for CAIX as a BC imaging target with promising prospects for clinical translation.

Disclosure Statement

The present study was funded by the National Natural Science Foundation of China [grant numbers 81771898 to Wanhai Xu].

References

1 Nguyen QT, Tsien RY: Fluorescence-guided surgery with live molecular navigation--a new cutting edge. Nat Rev Cancer 2013;13:653.
2 Garciaallende PB, Glatz J, Koch M, Ntziachristos V: Enriching the interventional vision of cancer with fluorescence and optoacoustic imaging. J Nucl Med 2013;54:664-667.
3 Atreya R, Goetz M: Molecular imaging in gastroenterology. Nat Rev Gastroenterol Hepatol 2013;10:704-712.
4 Siegel RL, Miller KD, Jemal A: Cancer Statistics, 2017 CA Cancer J Clin 2017;67:7-30.
5 Kamat AM, Hahn NM, Efstathiou JA, Lerner SP, Malmström PU, Choi W, Guo CC, Lotan Y, Kassouf W: Bladder cancer. Lancet 2016;388:2796.
6 Svatek RS, Hollenbeck BK, Holmäng S, Lee R, Kim SP, Stenzl A, Lotan Y: The economics of bladder cancer: costs and considerations of caring for this disease. Eur Urol 2014;66:253.
7 Babjuk M, Burger M, Zigeuner R, Shariat SF, van Rhijn BW, Comperat E, Sylvester RJ, Kaasinen E, Bohle A, Palou Redorta J, Roupret M: EAU guidelines on non-muscle-invasive urothelial carcinoma of the bladder: update 2013 Eur Urol 2013;64:639-653.
8 Witjes JA, Comperat E, Cowan NC, De Santis M, Gakis G, Lebret T, Ribal MJ, Van der Heijden AG, Sherif A: EAU guidelines on muscle-invasive and metastatic bladder cancer: summary of the 2013 guidelines. Eur Urol 2014;65:778-792.
9 Liu JJ, Droller MJ, Liao JC: New optical imaging technologies for bladder cancer: considerations and perspectives. J Urol 2012;188:361.
10 Lerner SP, Goh A: Novel endoscopic diagnosis for bladder cancer. Cancer 2015;121:169-178.
11 Daneshmand S, Schuckman AK, Bochner BH, Cookson MS, Downs TM, Gomella LG, Grossman HB, Kamat AM, Konety BR, Lee CT: Hexaminolevulinate blue-light cystoscopy in non-muscle-invasive bladder cancer: review of the clinical evidence and consensus statement on appropriate use in the USA. Nat Rev Urol 2014;11:589.
12 Potter C, Harris AL: Hypoxia inducible carbonic anhydrase IX, marker of tumour hypoxia, survival pathway and therapy target. Cell Cycle 2004;3:164.
13 Klatte T, Seligson DB, Rao JY, Yu H, De MM, Kawaoka K, Wong SG, Belldegrun AS, Pantuck AJ: Carbonic anhydrase IX in bladder cancer: a diagnostic, prognostic, and therapeutic molecular marker. Cancer 2009;115:1448.
14 Martino MD, Lucca I, Mbeutcha A, Wiener HG, Haitel A, Susani M, Shariat SF, Klatte T: Carbonic Anhydrase IX as a Diagnostic Urinary Marker for Urothelial Bladder Cancer. Eur Urol 2015;68:552.
15 Malentacchi F, Vinci S, Melina AD, Kuncova J, Villari D, Nesi G, Selli C, Orlando C, Pazzagli M, Pinzani P: Urinary carbonic anhydrase IX splicing messenger RNA variants in urogenital cancers. Urol Oncol Semin Orig Invest 2016;34:292.e299-292.e216.
16 Hanahan D, Weinberg RA: Hallmarks of cancer: the next generation. Cell 2011;144:646.
17 Höckel M, Vaupel P: Hockel, M. & Vaupel, P. Tumor hypoxia: Definition and current clinical, biologic, and molecular aspects. J Natl Cancer Inst 2001;93:266-276.
18 Trastour C, Benizri E, Ettore F, Ramaioli A, Chamorey E, Pouysségur J, Berra E: HIF-1alpha and CA IX staining in invasive breast carcinomas: prognosis and treatment outcome. Int J Cancer 2007;120:1451.
19 Kon-No H, Ishii G, Nagai K, Yoshida J, Nishimura M, Nara M, Fujii T, Murata Y, Miyamoto H, Ochiai A: Carbonic anhydrase IX expression is associated with tumor progression and a poor prognosis of lung adenocarcinoma. Lung Cancer 2006;54:409-418.
20 Loncaster JA, Harris AL, Davidson SE, Logue JP, Hunter RD, Wycoff CC, Pastorek J, Ratcliffe PJ, Stratford IJ, West CM: Carbonic anhydrase (CA IX) expression, a potential new intrinsic marker of hypoxia: correlations with tumor oxygen measurements and prognosis in locally advanced carcinoma of the cervix. Cancer Res 2001;61:6394.
21 Stillebroer AB, Mulders PF, Boerman OC, Oyen WJ, Oosterwijk E: Carbonic anhydrase IX in renal cell carcinoma: implications for prognosis, diagnosis, and therapy. Eur Urol 2010;58:75-83.
22 Ashida S, Nishimori I, Tanimura M, Onishi S, Shuin T: Effects of von Hippel-Lindau gene mutation and methylation status on expression of transmembrane carbonic anhydrases in renal cell carcinoma. J Cancer Res Clin Oncol 2002;128:561.

23 Burger M, Grossman HB, Droller M, Schmidbauer J, Hermann G, Drăgoescu O, Ray E, Fradet Y, Karl A, Burgués JP: Photodynamic Diagnosis of Non–muscle-invasive Bladder Cancer with Hexaminolevulinate Cystoscopy: A Meta-analysis of Detection and Recurrence Based on Raw Data. Eur Urol 2013;64:846-854.
24 D'Hallewin MA, Vanherzeele H, Baert L: Fluorescence Detection of Bladder Cancer. Eur Urol 2002;42:417.
25 Ray ER, Chatterton K, Khan MS, Chandra A, Thomas K, Dasgupta P, O'Brien TS: Hexylaminolaevulinate fluorescence cystoscopy in patients previously treated with intravesical bacille Calmette-Guérin. BJU Int 2010;105:789.
26 Jichlinski P, Guillou L, Karlsen SJ, Malmström PU, Jocham D, Brennhovd B, Johansson E, Gärtner T, Lange N, Bergh HVD: Hexyl Aminolevulinate Fluorescence Cystoscopy: A New Diagnostic Tool for Photodiagnosis of Superficial Bladder Cancer—A multicenter study. J Urol 2003;170:226-229.
27 Steinbach P, Wedmgandt H, Baumgartner R, Kriegmair M, Hofstädter F, Knüchel R: Cellular fluorescence of the endogenous photosensitizer protoporphyrin IX following exposure to 5-aminolevulinic acid. Photochem Photobiol 1995;62:887.
28 Lamm DL, Blumenstein BA, Crissman JD, Montie JE, Gottesman JE, Lowe BA, Sarosdy MF, Bohl RD, Grossman HB, Beck TM: Maintenance bacillus Calmette-Guerin immunotherapy for recurrent TA, T1 and carcinoma in situ transitional cell carcinoma of the bladder: a randomized Southwest Oncology Group Study. J Urol 2000;163:1124.
29 Kamat AM, Orten S: Myths and Mysteries Surrounding Bacillus Calmette-Guérin Therapy for Bladder Cancer. Eur Urol 2014;65:267-269.
30 Wu C, Zhou X, Miao C, Zhang J, Tang Q, Chang X, Ni H: Assessing the Feasibility of Replacing Standard-Dose Bacillus Calmette-Guérin Immunotherapy with Other Intravesical Instillation Therapies in Bladder Cancer Patients: A Network Meta-Analysis. Cell Physiol Biochem 2017;41:1298.
31 Chang DK, Moniz RJ, Xu Z, Sun J, Signoretti S, Zhu Q, Marasco WA: Human anti-CAIX antibodies mediate immune cell inhibition of renal cell carcinoma *in vitro* and in a humanized mouse model *in vivo*. Mol Cancer,14, 1(2015-06-11) 2015;14:119.
32 Suarez ER, Chang DK, Sun J, Sui J, Freeman GJ, Signoretti S, Zhu Q, Marasco WA: Chimeric antigen receptor T cells secreting anti-PD-L1 antibodies more effectively regress renal cell carcinoma in a humanized mouse model. Oncotarget 2016;7:34341.
33 Eisen T, Sternberg CN, Robert C, Mulders P, Pyle L, Zbinden S, Izzedine H, Escudier B: Targeted therapies for renal cell carcinoma: review of adverse event management strategies. J Natl Cancer Inst 2012;104:93.
34 Nan Z, Ling Z, Ruan YF, Zhao WW, Xu JJ, Chen HY: Quantum-dots-based photoelectrochemical bioanalysis highlighted with recent examples. Biosens Bioelectron 2017;94:207.
35 Hesse AR, Levent E, Zieseniss A, Tiburcy M, Zimmermann WH, Katschinski DM: Lights on for HIF-1α: genetically enhanced mouse cardiomyocytes for heart tissue imaging. Cell Physiol Biochem 2014;34:455.
36 Chang SG, Lee SJ, Lee CH, Jin IK, Kim YW: Expression of human erythrocyte glucose transporter in transitional cell carcinoma of the bladder. Urology 2000;55:448-452.
37 Peng L, Xiao Y, Cheng Y, Zhang X, Yang C, Deng X, Li P, Tao J, Yang H, Wei J: MicroRNA-218 Increases the Sensitivity of Bladder Cancer to Cisplatin by Targeting Glut1. Cell Physiol Biochem 2017;41:921.
38 Martin TA, Harrison G, Mansel RE, Jiang WG: The role of the CD44/ezrin complex in cancer metastasis. Crit Rev Oncol Hematol 2003;46:165.
39 Fang M, Wu J, Lai X, Ai H, Tao Y, Zhu B, Huang L: CD44 and CD44v6 are Correlated with Gastric Cancer Progression and Poor Patient Prognosis: Evidence from 42 Studies. Cell Physiol Biochem 2016;40:567.
40 Yang N, Zhou TC, Lei XX, Wang C, Yan M, Wang ZF, Liu W, Wang J, Ming KH, Wang BC: Inhibition of Sonic Hedgehog Signaling Pathway by Thiazole Antibiotic Thiostrepton Attenuates the CD44+/CD24-Stem-Like Population and Sphere-Forming Capacity in Triple-Negative Breast Cancer. Cell Physiol Biochem 2016;38:1157-1170.
41 Klatte T, Seligson DB, Rao JY, Yu H, De MM, Garraway I, Wong SG, Belldegrun AS, Pantuck AJ: Absent CD44v6 expression is an independent predictor of poor urothelial bladder cancer outcome. J Urol 2010;183:2403.
42 Pan Y, Volkmer JP, Liu JJ, Sahoo D, Chang T, Mach K, Rouse R, Freiha F, Gambhir S, Weissman I: Endoscopic molecular imaging of human bladder cancer using a CD47 antibody. Sci Transl Med 2014;6:260ra148.